Article

Desorption of HO from Flat and Stepped Pt(111)

Alexander Picolin, Carsten Busse, Alex Redinger, Markus Morgenstern, and Thomas Michely

More About This Article

Additional resources and features associated with this article are available within the HTML version:

- Supporting Information
- Access to high resolution figures
- Links to articles and content related to this article
- Copyright permission to reproduce figures and/or text from this article

View the Full Text HTML

Desorption of H₂O from Flat and Stepped Pt(111)

Alexander Picolin,[†] Carsten Busse,*,[†] Alex Redinger,[†] Markus Morgenstern,[‡] and Thomas Michely[†]

II. Physikalisches Institut, Universität zu Köln, 50937 Köln, Germany, II. Physikalisches Institut B, RWTH Aachen, 52056 Aachen, Germany

To investigate the effect of steps on H₂O binding on a nominal Pt(111) surface, we used thermal desorption spectroscopy of water adsorbed on purposefully nanostructured surfaces: a rippled surface containing densely packed (100)-microfaceted and (111)-microfaceted steps was created using grazing incidence ion bombardment, and a surface with triangular mounds mainly consisting of (111)-microfaceted steps was fabricated through homoepitaxial growth. These morphologies are determined by scanning tunneling microscopy. We find two additional high-temperature H₂O desorption peaks using the rippled surface, whereas only the peak with the highest desorption temperature is present on the (111)-microfaceted mound. Thus, water preferentially binds to steps and especially favors (111)-microfaceted ones. Furthermore, the large step concentration on our nanostructured surfaces precludes the coexistence of a condensed and a diluted phase in a monolayer of water and suppresses the formation of crystalline ice multilayers during heating.

1. Introduction

The interaction of water with solid surfaces is of utmost importance in both technologically important fields and in our environment. To name a few: it is the foundation of electrochemical processes in aqueous solution,[1] it lies at the heart of corrosion processes,[2] it governs the formation of ice particles in the stratosphere,[3] and it is important in interstellar chemistry.[4] To reveal the underlying principles of the interaction of water with solid surfaces, numerous studies have been undertaken in recent years in which the interaction of H₂O with model surfaces was studied using surface science methods.[5–7] An especially well studied system is the interaction of water with closely packed surfaces of noble or transition metals, the most prominent example being Pt(111) (see, e.g., refs 8–15).

Although in model studies, flat and defect-free surfaces are the center of attention, it is obvious that crystal imperfections such as surface steps have a nonnegligible contribution to the adsorption behavior because steps are typically more reactive than terrace sites and, thus, can be of decisive influence for adsorption and surface reactions. These defects are always present in a small concentration on a nominally flat single-crystal surface. Even more important, in less academic systems, such as polycrystalline surfaces or for small particles, defects sites (e.g., step sites) form a large fraction of the total surface area.

In the work presented here, we will analyze the influence of steps on the adsorption and desorption of H₂O using thermal desorption spectroscopy (TDS). In contrast to other studies, we did not use single crystals with surfaces vicinal to high-symmetry surfaces, but instead, we employ nanostructuring of a Pt(111) sample. Using ion bombardment or homoepitaxial growth, we are able to produce surface morphologies locally corresponding to different vicinal surfaces. In doing so, we avoid laborious preparation of a whole set of crystals. At the same time, the experiments on different surface morphologies are directly comparable to each other because they are obtained in one experimental series without sample exchange. Mandatory for this approach is a reliable characterization of the morphology on the local scale, which we achieved in this study using scanning tunneling microscopy (STM). Before describing our work in detail, we will briefly summarize the relevant knowledge on H₂O/Pt(111).

Water adsorbs molecularly on Pt(111),[10] and single molecules are bound on on-top positions via O−Pt bonds.[12] Subsequent deposition of a full monolayer at temperatures where water effectively diffuses ($T > 60$ K[8,13]) leads to the formation of a hydrogen-bonded wetting layer. This structure is composed of connected ice rings in which, in additon to bonding to three neighbors in the hexagonal pattern, half of the molecules are bound to the surface via O−Pt bonds, whereas the other half is bound via O−H−Pt bonds[10] (H-down model), making every water molecule four-fold coordinated. This is in contrast to bulk ice, in which bonds are available to bind the next water layer. As a consequence, the monolayer offers no chemical binding to subsequent layers, making it hydrophobic.[14,15] The detailed structure of the monolayer depends on the exact preparation method and the total water coverage. For full coverage, measurements by He atom scattering[9] and LEED[11] yielded a ($\sqrt{39} \times \sqrt{39}$)R16.2° structure, whereas for lower coverages, a ($\sqrt{37} \times \sqrt{37}$)R25.3° structure was found.[9] An additional structure was found using STM.[16]

Temperature-dependent specular He scattering[13] has shown that desorption from the monolayer is a zero-order process with a desorption barrier $E^{\text{flat}}_{\text{terrace}} = (560 \pm 30)$ meV and a frequency factor of $\nu^{\text{flat}}_{0,\text{terrace}} = (1.4 \pm 3.5) \times 10^{16}$ s⁻¹. Only a single peak for the desorption of the monolayer is observed in several studies[13,11,14] at temperatures in the range of 160−170 K.

The film structure after subsequent growth of a few more layers on top of this wetting layer depends on growth temperature and growth rate:[11] at low temperature ($T < 135$ K), amorphous solid water is formed on top of the hydrophobic wetting layer. For high temperatures ($T \geq 137$ K), the crystalline monolayer acts as a template, and the first few layers adopt to

* Corresponding author. Phone: +49-221-470-3599. Fax: +49-221-470-5178. E-mail: busse@ph2.uni-koeln.de.
† Universität zu Köln.
‡ RWTH Aachen.
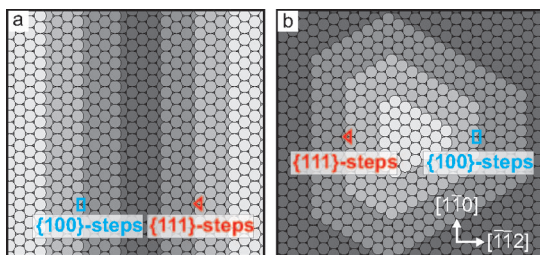
Figure 1. Ball model of the nanostructured Pt(111) surface representing step arrangements used in this study. (a) Ripple as produced by grazing incidence ion bombardment along [1$\bar{1}$0]. The side walls are locally equivalent to Pt(335) (left-hand side) containing (100)-microfaceted steps (blue rectangles) and Pt(221) (right-hand side) containing (111)-microfaceted steps (red triangles). (b) Mound as produced by homoepitaxial growth. It is predominantly bounded by (111) steps. For simplicity, this structure will be called a triangular mound.

this structure. Upon heating (or upon growth of thicker films for the crystalline monolayer), both structures (re)crystallize into bulk ice,[17,11,18] which is incommensurate with Pt(111).

For amorphous solid water films, desorption takes place as a zero-order process.[19] The multilayer desorption signal consists of a main peak (at a sample temperature of $T \approx 155$ K[11]) and a shoulder (around $T = 152$ K[17,19]). This peak structure is attributed to the crystallization of amorphous solid water during heating, which leads to the formation of crystalline ice with a slightly lower vapor pressure. Consequently, for crystalline ice films grown at a higher temperature, no shoulder is observed upon heating.[11]

There is evidence that water molecules preferentially bind to steps on Pt(111). On one hand, STM measurements[20] show that annealing (2 min at 160 K) of a monolayer desorbs all water except chains along both types of densely packed steps (steps in the ⟨1$\bar{1}$0⟩ direction with either (100) microfacets (also called A-steps) or (111) microfacets (B-steps), see Figure 1). Density functional theory (DFT) calculations indicate that water molecules form one-dimensional, hydrogen bonded chains along step edges.[21,22] On a vicinal Pt(335) surface (four-atom-wide Pt(111) terraces bounded by (100)-steps, alternative notation Pt(533)), a combined TDS and reflection adsorption infrared spectroscopy study[21] shows that already for very low coverages, H_2O forms hydrogen bonded molecular chains along the step edges, in accordance with high resolution electron energy loss spectroscopy (HREELS) measurements on a flat surface containing a significant number of defects.[23]

A few earlier studies reported additional signals in the TDS for higher temperatures; namely, a peak/shoulder at $T \approx 198$ K,[24,25] which has been tentatively assigned to desorption from step edges.[20] This issue was clarified by a study on a vicinal Pt(335) surface, which clearly revealed a peak at $T = 198$ K due to molecules bound to step edges in addition to the multilayer ($T = 160$ K) and monolayer peak ($T = 185$ K).[21] A further source for additional high temperature desorption peaks is the presence of OH, which tends to stabilized, mixed OH–H_2O overlayer on Pt(111).[26]

2. Experimental Methods

The experiments were performed in an ultrahigh vacuum variable temperature apparatus with a base pressure in the 10^{-11} mbar range[27] containing a gas dosing system and a shielded mass spectrometer to perform TDS and a home-built beetle STM. Sample cleaning was accomplished by cycles of ion bombardment (5 keV Ar⁺), exposure to 10^{-6} mbar of oxygen at $T = 773$ K, and flash annealing to 1273 K.

A highly stepped (rippled) surface was created by ion bombardment under a grazing incidence angle of $\theta = 83°$ with respect to the surface normal along the [1$\bar{1}$0] direction at $T = 450$ K. An ion fluence around 100 MLE (monolayer equivalents; 1 MLE is an ion fluence identical to the surface atomic density, i.e. 1.504×10^{19} ions/m² for Pt (111)) leads to the formation of ripples parallel to the ion beam.[28,29]

For homoepitaxial growth, atoms were evaporated from a resistivity-heated Pt wire (purity 99.99%) with a rate of 4×10^{-3} ML/s. Clean (i.e., CO-free) conditions are established by performing the growth in an oxygen background (partial pressure $p_{O_2} = 9.2 \times 10^{-9}$ mbar) reacting away any CO.

Water (Ultrapur from Merck, additionally cleaned by freeze–pump–thaw cycles) was provided in a gold-plated reservoir (volume $V = 28$ cm³) filled to a pressure of 5×10^{-3} mbar as determined using a chemically inactive spinning rotor gauge. It was delivered to the surface through a leak valve feeding a glass tube directed toward the sample. Immediately before H_2O adsorption, the sample was briefly heated to 560 K to ensure that steps and kinks are free of CO. The adsorption rate employed here was $R = 0.01$ ML/s in the center of the sample[30] and adsorption took place at a sample temperature of $T \approx 130$ K. One monolayer (ML) of H_2O is defined as the layer that contains all molecules bound directly to the metal surface through either Pt–O or PT–H–O bonds (this layer is sometimes called the bilayer, implicating that it has a buckled structure, as in bulk ice). Choosing as a reference the ($\sqrt{39} \times \sqrt{39}$)R16.1° structure with respect to Pt(111),[9] this is equivalent to 1.23×10^{19} molecules/m⁻².[18] CO is let in through a secondary gas system, leading to a stainless steel tube ending close to the sample. The gas pressure at the sample is enhanced by a factor of ≈35 with respect to the chamber pressure far away from the gas inlet, as determined by measuring the CO coverage via the monolayer peak in CO desorption. CO dosing was performed using a chamber pressure of 3×10^{-9} mbar.

TDS measurements were obtained using a shielded quadrupole mass spectrometer (aperture with a radius of 2.5 mm at a distance of 5 mm from the surface). The mass spectrometer signal at $m = 18$ u was recorded as a function of temperature. The thermally well isolated sample was cooled with liquid nitrogen and heated by electron bombardment from a tungsten filament using a heating rate of $\beta = 0.67$ K s⁻¹. Sample temperature was measured by a NiCr–Ni thermocouple spot-welded to the sample. The error in temperature measurement is below 3 K. The raw spectra were FFT-smoothed (cutoff frequency $\nu = 0.75$ K⁻¹) and a background consisting of two continuously merged straight lines was subtracted.

3. Results

A surface morphology with a high density of steps is created on Pt(111) by ion bombardment under grazing incidence.[28,29] A fluence of 90 MLE of 5 keV Ar⁺ leads to the morphology shown in Figure 2a. The facets formed are approximately (335) containing only (100)-steps (left side wall of the ripple as seen from the valley) and (221) containing only (111)-steps (right side wall), both with a (111)-terrace width of four rows (see Figure 1). The average distance between two ripples is ≈110 Å, and the top of the ripples is a flat terrace of ≈16 Å width. This leads to an overall step edge atom density of 26%, of which 13% belong to (100) steps and 13% to (111) steps.

TDS on the rippled surface yields the spectra shown in Figure 3b. On the basis of previous experiments, we identify peak A as the multilayer peak and peak B as the monolayer peak. The spectra are significantly different from those obtained on the
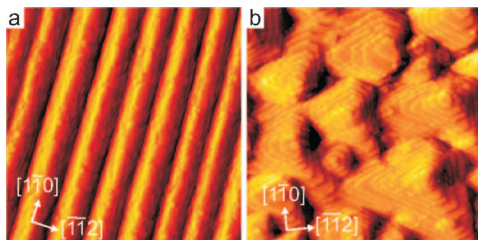
Figure 2. (a) STM topograph of a rippled Pt(111) surface. Grazing incidence ion bombardment (90 MLE) creates a highly stepped surface with an equal number of (100) and (111) steps. Scan width 900 Å. (b) STM topograph of a Pt(111) surface with mounds. After evaporation of ≈30 ML Pt at 425 K, triangular mounds have formed, predominantly bounded by (111) steps. Scan width 900 Å. Both images are taken in the differentiated mode and appear as if illuminated from the left.

flat surface (see Figure 3a) and already demonstrate the main findings in this paper, which will be treated in detail below: (i) two new high-temperature peaks appear (C, D); (ii) the monolayer peak is shifted and has a different peak shape; and (iii) the multilayer signal on the rippled surface contains only one peak (A), whereas it has a double peak structure on the flat surface (main peak A_2 and a shoulder A_1).

At high temperatures, two new peaks appear in the desorption spectra: one at $T_{max, C} = 187$ K, labeled peak C; and one at $T_{max, D} = 194$ K, labeled peak D. Following the spectra shown in Figure 3b starting from the lowest H₂O exposures reveals that peak D is populated first, followed by peak C. The peak positions do not shift with coverage, indicating first-order desorption.

Since the two new peaks appear only on a highly stepped surface, we attribute them to an adspecies related to the presence of steps. To strengthen this interpretation, we performed additional experiments in which we passivated the Pt(111) steps using CO. This was achieved by exposing the surface to ≈5 L at a temperature of 400 K, where CO desorption from step edges is negligible. Because it is well-known that CO preferentially binds to step edges,[31] this procedure leads to a passivation of all step edge atoms.

TDS measurements including CO passivation are shown in Figure 3d. The rippled surface prepared as above (solid black line in Figure 3d) shows an H₂O desorption spectrum identical to those in Figure 3b. Passivating the surface using CO and renewed water adsorption leads to the spectrum shown in red. Here, the additional peaks C and D are absent, whereas the monolayer peak B is shifted to lower temperatures (from 173 to 169 K), as was previously observed for the case of CO/H₂O coadsorption.[32] Subsequent heating of the sample (flash to 560 K) above the desorption temperature of CO (also from steps) restores the clean surface.[33] The respective H₂O-desorption spectra (dashed black line in Figure 3d) are again qualitatively identical to the spectra obtained on the clean rippled surface.

These findings corroborate our interpretation of peaks C and D as step-edge-related peaks. To investigate this relationship further, we prepared a surface containing preferentially only one type of step. This is achieved by multilayer growth under clean conditions at a sample temperature of 425 K, which is known to produce mounds with a triangular shape consisting mainly of (111) steps.[31] Depositing ≈30 ML leads to the morphology shown in Figure 2b. The density of step edge atoms as determined from such topographs is $(7.9 \pm 0.4)\%$ for (111) steps and $(2.6 \pm 0.2)\%$ for (100) steps. The side walls of the mounds are not as steep as for the ripples and can be approximated by a (997) surface with a terrace width of nine rows. The desorption
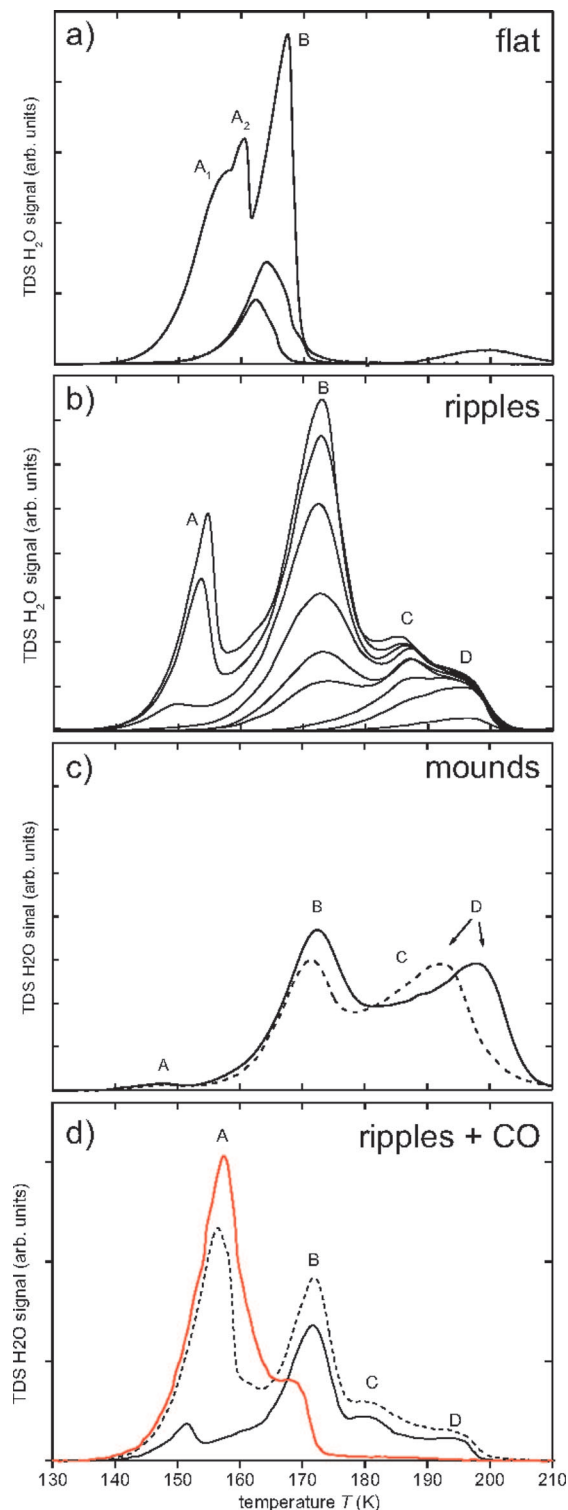
Figure 3. TDS of H₂O on Pt(111) with varying surface morphologies. (a) Flat surface, initial coverages between 0.3 and 1.8 ML. (b) Rippled Pt(111) surface similar to the one shown in Figure 2a prepared using a fluence of ≈100 MLE. Initial H₂O coverages range from 0.04 to 1.5 ML. (c) Pt(111) surface containing triangular mounds (similar to the one shown in Figure 2b), initial coverages around 0.5 ML. Solid line: spectra after preparation of mounds, one flash to 560 K, and water adsorption. Dashed line: Desorption signal after second flash to 560 K and renewed water adsorption. (d) Rippled Pt(111) surface prepared by grazing incidence ion bombardment (fluence ≈ 100 MLE) including CO-passivation with initial H₂O coverages around 1.5 ML. Solid black line, initial preparation (free of CO); red, CO-passivated surface; dashed black, recovered clean surface (flash to 560 K).

TABLE 1: Experimentally Determined Desorption Parameters

morphology	peak	T_{max} [K]	m	E [meV]	E [kJ/mol]	ν_0 [s^{-1}]
flat	A_1	156−162	0	500 ± 30	48 ± 3	$1.0 \times 10^{15\pm0.8}$
	B	160−168	0	550 ± 40	53 ± 4	$3.1 \times 10^{15.0\pm1.3}$
rippled	A	154−155	0	520 ± 30	50 ± 2	$6.5 \times 10^{15.0\pm0.8}$
	B	174	1	560 ± 20	54 ± 2	$[3.1 \times 10^{15}]$
	C	187	1	610 ± 20	59 ± 2	$[3.1 \times 10^{15}]$
	D	194	1	640 ± 20	61 ± 2	$[3.1 \times 10^{15}]$

Desorption order, m; desorption energy, E; and frequency factor, ν_0 for the different peaks studied here. The peaks of order zero were analyzed using eq 2. All other peaks were evaluated on the basis of the Redhead equation (eq 3) assuming the frequency prefactor $\nu_1^0 = 3.1 \times 10^{15.0\pm1.3}$ determined for monolayer desorption on the flat surface. For the multilayer peak on the flat surface, T_{max} refers to the high component A_2, whereas the parameters were obtained from the common leading edge of the shoulder A_1.

signal for such a surface is shown in Figure 3c. The spectrum taken directly after the film growth and a first annealing to 560 K (full line in Figure 3c) shows the monolayer peak B as well as the step-edge peak D at high temperatures, but not the second step edge peak C (compare the curves obtained on the rippled surface). A similar behavior is observed for the second spectra taken after annealing to 560 K and renewed water adsorption on the surface containing mounds (dashed line in Figure 3c), but here, already a deterioration of the spectra sets in due to thermally activated rounding of the mounds at the annealing temperature.

In the following, we will describe the effect of the highly stepped surface on the monolayer peak. With a higher initial coverage, the monolayer peak B appears in the TDS signal in Figure 3b. Analysis of the peak position shows that it is always found at the same temperature of 170.0 ± 0.2 K. In addition, a small shoulder is visible at $T \approx 165$ K. The constant peak temperature indicates first-order desorption, in contrast to the flat surface, where we find that the monolayer desorption peak B shows a common leading edge for different initial water coverages (see Figure 3a), indicating zero-order desorption in accordance with literature. The different desorption orders are also evident in the different peak shapes for the monolayer peak B on the flat and on the rippled surface. In the case of zero-order desorption, as found on the flat surface, the first part of the peak can be analyzed to yield the desorption parameters E (energy barrier against desorption) and ν_0 (frequency prefactor) using the Wigner−Polanyi equation,

$$-\frac{d\Theta}{dT} = \Theta^m \times \frac{\nu_0}{\beta} \times e^{-\frac{E}{k_B T}} \qquad (1)$$

Here, Θ is the coverage, $-(d\Theta)/(dT)$ is the desorption rate, and m is the order of the desorption. In the case of zero-order desorption, this can be written as

$$\ln\left(-\frac{d\Theta}{dT}\right) = \ln\left(\frac{\nu_0}{\beta}\right) - \frac{E}{k_B} \times \frac{1}{T} \qquad (2)$$

As a consequence, a plot of $\ln(-(d\Theta)/(dT))$ vs $1/T$ directly yields E from the slope and ν_0 from the y-axis interception for zero-order desorption processes.

Applying this procedure to the monolayer peak B on the flat surface yields $E_{terrace}^{flat} = 550 \pm 40$ meV and $\nu_{0,\,terrace}^{flat} = 3.1 \times 10^{15.0\pm1.3}$ s^{-1} (see Table 1).

In the case of a first-order desorption process, as found for the monolayer peak B on the stepped surface, we can evaluate the desorption parameters via the Redhead equation,[34]

$$E = k_B T_{max}\left[\ln\left(\frac{\nu_0 \times T_{max}}{\beta}\right) - 3.64\right] \qquad (3)$$

For the frequency prefactor, ν_0, we use the value determined for the monolayer peak on the flat surface. This leads to $E_{terrace}^{stepped} = 560 \pm 20$ meV. On first sight, it may seem questionable to use the same prefactor for a zero- and a first-order process. However, as will be detailed below in the Discussion, exactly this behavior was found in a high-resolution TDS study for Xe on Pt(997).[35] Applying the same procedure to the step peaks C and D leads to $E_C^{stepped} = 610 \pm 20$ meV for peak C and $E_D^{stepped} = 640 \pm 20$ meV for peak D.

For the highest initial water coverages presented in Figure 3b, a multilayer peak A starts to grow. The leading edge of the multilayer peak is the same for different initial H_2O coverages. This indicates that the desorption process is of zero order. Proceeding as above (eq 2) leads to a desorption energy of $E_{multi}^{stepped} = 520 \pm 30$ meV and a frequency factor of $\nu_{0,\,multi}^{stepped} = 6.5 \times 10^{15.0\pm0.8}$ s^{-1}.

In contrast to the single multilayer peak A observed on the stepped surface, on the flat surface, the multilayer peak A is a double peak (A_1 and A_2, see Figure 3a). For the highest coverages employed, the spectra have a common leading edge in the region of A_1, indicating zero-order desorption, as observed on the stepped surface. Applying eq 2 to the shoulder of the multilayer peak A_1 leads to $E_{multi}^{flat} = 500 \pm 30$ meV and $\nu_{0,\,multi}^{flat} = 1.0 \times 10^{15.0\pm0.8}$ s^{-1}.

4. Discussion

In principle, several models are able to explain our finding of new desorption peaks for highly stepped surfaces. It could be caused by water molecules bound with a higher binding energy in the vicinity of the steps.[20,23,22] An alternative explanation is step-induced dissociative adsorption of water molecules, since the steps are chemically more active than the flat surface, where water adsorbs intact. The presence of OH is known to cause high-temperature desorption peaks for H_2O/Ru(0001)[36] or mixed OH−H_2O adlayers on Pt(111).[26]

A strong clue to the correct interpretation of our measurements is the fact that we observe *two* new peaks for the case of the rippled surface, in contrast to only *one* clearly visible peak in the case of the surface containing mounds. To quantify this observation, we evaluated the relative populations of these peaks for both the rippled surface and the surface containing mounds. Therefore, we used the experimentally determined parameters from Table 1 to fit peaks C and D with the Wigner−Polanyi equation (eq 1), using a numerical approximation up to fourth order to the respective Arrhenius integral.[37,38] The remaining signal is then attributed to peak B (see Figure 4). For the rippled surface (Figure 4a), the integral over the deconvoluted peaks as a measure of step coverage leads to $\Theta_C/\Theta_D \approx 1.0$. Since in the experiments depicted in Figure 4 the initial coverage was high enough to saturate all surface steps, this ratio should be identical to the ratio of (100) steps to (111) steps, which indeed is (100) steps/(111) steps = 1 (remember Figure 1), inherent for the rippled surface. For the surface containing triangular mounds (Figure 4b), the distribution of intensity within peaks C and D is not symmetrical ($\Theta_C/\Theta_D \approx 0.4$), corresponding to the asymmetry in step type distribution observed on this surface ((100) steps/(111) steps = 0.3).

This finding indicates that the two step edge peaks C and D stem from an adsorbed species bound with different binding energies at the two different types of closely packed steps, with the highest binding energy present at the (111) steps. Still, it is
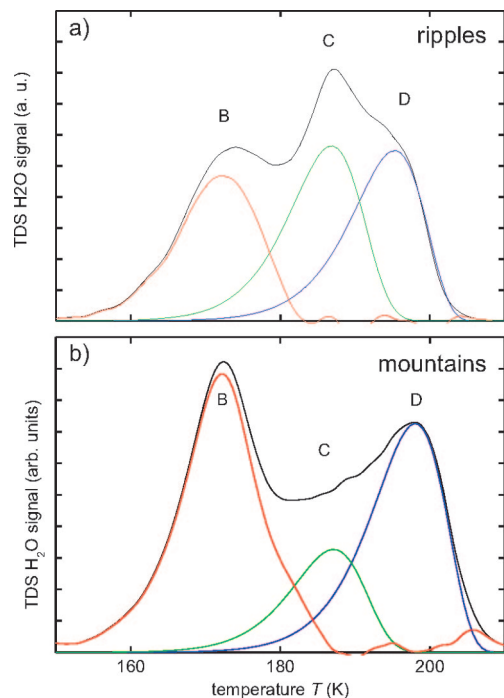
Figure 4. Deconvoluted TDS signals of H₂O on Pt(111) surfaces with different morphologies. (a) Rippled surface; compare to Figure 3b. (b) Surface containing triangular mounds; compare to Figure 3c. The initial coverages are in both cases around 0.5 ML. The spectra are deconvoluted to separate peaks B, C, and D by fitting them with the Wigner−Polanyi equation (1) using the experimentally determined parameters (Table 1).

not certain whether the adsorbed species are water molecules or OH groups created by dissociative adsorption at the chemically active steps. However, DFT calculations comparing intact and dissociative adsorption at (100) steps come to the conclusion that dissociative adsorption is energetically unfavorable. Therefore, we conclude that peak C is due to H₂O adsorbed at (100) steps with a somewhat lower binding energy, and peak D is due to molecules adsorbed at (111) steps with a significantly higher binding energy. This interpretation is further corroborated by the fact that for CO on vicinal Pt(111), the same order of adsorption for the different step types was found.[33]

The fact that for low coverages on a rippled surface only a desorption signal from (111) steps is observed indicates that the diffusion of the molecules must be rather effective because the rippled surface facets containing different step types are separated by 12 nm. Furthermore, this indicates that molecules are able to cross (several) step edges. This finding is in accordance with literature: An early theoretical analysis revealed a diffusion barrier for H₂O monomers of $E_{\text{d, monomer}} = 30$ meV,[39] corroborated by experimental findings that monomer diffusion is already active at 20 K.[8] Lacking an experimental or theoretical value for the detachment of step-bound water, we employ a simple model and assume that in addition to the diffusion barrier for a monomer, the difference in binding energy between a molecule adsorbed at the step and a molecule adsorbed on a terrace has to be overcome to make one diffusion step. A recent DFT calculation[40] establishes a binding energy of a molecules inside a molecular chain at a (100) step as $E_{\text{b,(100)−step chain}} = 480$ meV. Together with the binding energy of a monomer on the flat terrace ($E_{\text{b, terrace}} = 304$ meV), this yields a difference of $E_{\text{b, terrace}} - E_{\text{b,(100)−step chain}} = 176$ meV. Together with the simple model introduced above, this leads to a diffusion barrier for a molecule to leave such a molecular chain of

$E_{\text{d,(100)−step chain}} \approx 210$ meV. Using for simplicity the same prefactor of $\nu_0 = 3.1 \times 10^{15}$ s⁻¹ as determined for the desorption from the monolayer on the flat surface, this process is activated (i.e., happens with a frequency of 1 Hz) at a temperature of ≈70 K, well below the adsorption temperatures used here. Looking at a (111) step where the molecules are bound a little bit stronger will not change this value much. Therefore, we conclude that already at our adsorption temperature of around 130 K, the potential minima at the step edges are not deep enough to trap the molecules. An additional barrier for diffusion across a step (an Ehrlich−Schwoebel barrier) might be present in this system. However, our measurements show that it is not high enough to prevent diffusion across step edges. Thus, the molecules will be distributed among the different step types and the terrace probably according to a Boltzmann distribution. Assuming this distribution, the energy difference deduced from our TPD experiments (see Table 1) is large enough so that population of adsorption states with a lower binding energy is below 15% at the measured desorption temperatures so long as states with a higher energy are still available. The fact that molecules can effectively exchange between steps and terraces does not contradict the finding of well-separated step-edge desorption peaks as has been demonstrated by measurements in the system CO/Pt(111).[41]

Our experiments lead us to the following picture: Upon adsorption at $T \approx 130$ K, the water molecules diffuse freely on the surface and are able to find the positions with the highest binding energy, which are the (111) steps. Nucleation of ice islands on terraces does not take place because the distance between steps is much smaller than the characteristic separation of islands on the flat surface. As long as the amount of water deposited is not enough to saturate this type of binding site, population of other sites is small. The molecules will desorb from (111) steps, giving rise to the appearance of peak D as the signal arising first in the spectra. Dosing more water also populates (100) steps, in turn yielding the second step-edge-related peak in the spectra.

The preferential binding of water molecules is, of course, due to the altered electronic structure at step edges. This enhanced interaction has been reproduced in DFT calculations,[22,21] but no detailed picture of the charge transfer between molecule and surface has been given yet. In a previous publication,[20] some of us explained the preference for steps by the reduced density of occupied Pt 5d states at the step. Because the main component of the H₂O−Pt bond is the charge transfer from the full sp shells of H₂O into these 5d states, the bond strength is consequently increased at steps. A theoretical treatment of the differences between the two types of closed packed steps is still missing. In ref 20, a higher adsorption density of water molecules above the (100) step was observed using STM, and it was tentatively assumed that this behavior indicates stronger binding to the (100) steps, in contrast to the findings presented here. However, such an effect could also be caused by different nucleation kinetics at the two different step types. In ref 20, the speculation was presented that that the amount of charge transfer away from the step can be inferred from the step dipole moment, which is 20% higher for (100) steps as compared with (111) steps,[42] implicating stronger bonding of water to (100) steps. In view of our measurements presented here, we have to conclude that the simplified treatment from ref 20 is not sufficient to explain the subtle differences in H₂O binding to the two different step types on Pt(111).

In the rest of this section, we will discuss our results concerning the remaining two effects of the high step density;

namely, the changed kinetic order for the desorption of the monolayer and the disappearance of the shoulder in the multilayer peak. As established in the literature, we observe a zero-order desorption process for the monolayer on the flat surface. This is usually explained by a phase coexistence between a condensed and a diluted phase, leading to a coverage-independent chemical potential and, consequently, to a zero-order desorption process.[13] The determined desorption energy of $E_{mono}^{flat} = 550 \pm 40$ meV is in accordance with literature values of $E_{mono}^{flat} = 540 \pm 20$ meV[11] and $E_{mono}^{flat} = 560 \pm 30$ meV.[13] Previous experiments also determined a frequency factor of similar magnitude ($\nu_0 \approx 10^{16}$ s^{-1} [13]), as observed here ($\nu_0 = 3.1 \times 10^{15.0 \pm 1.3}$ s^{-1}).

In contrast, on the rippled surface, desorption from the terraces is of first order. This is understandable if one assumes that on the small terraces, phase coexistence cannot be established; that is, only one phase of H_2O is present on small terraces. The same behavior has been reported for Xe on Pt(997),[35] where TDS supported by lattice-gas calculations showed that Xe desorption in the submonolayer regime on Pt(111) is a zero-order process, but on stepped Pt(997), it is of first order. The desorption parameters found in this high-resolution study for these two processes were identical, making our assumption of the same frequency prefactor for both the flat and the stepped surface plausible.

The desorption from terraces on the flat and highly stepped surface has energy barriers which are identical within their error bars. This indicates that both species desorb via a similar pathway. Thus, we do not observe an effect of the presence of steps on the binding energy on terraces; only the order of the desorption process is significantly changed, which is the main contribution to the different appearance of these two peaks in our measurements (see Figure 3b). This finding is in contrast to the results of Grecea et al.[21] The small shoulder visible for the monolayer peak on the rippled surface is attributed to the presence of the terraces on top of the ripples, where a behavior similar to the flat surface is expected because these plateaus are rather extended and not bound by ascending steps.

On the surface containing mounds, the desorption signal of the terrace molecules is similar to the one observed on the rippled surface (see Figure 3b). This indicates that the larger average terrace width present there (nine rows, as compared with four rows on the rippled surface) is still not sufficient to allow phase coexistence.

The desorption energy of the multilayer peak on the flat surface of $E_{multi}^{flat} = 500 \pm 30$ meV is in the energy range of the well-known sublimation enthalpy of ice[43] ($E_{subl} = 530$ meV), but the mean is significantly lower. This can be attributed to the fact that we are looking at desorption from an amorphous solid water layer, which is less stable than crystalline ice. For the desorption of crystalline ice multilayers on Pt(111), a value of $E_{multi}^{flat} = 520 \pm 20$ eV has been reported previously.[11]

The peak shape of the multilayer peak on the flat surface (see Figure 3b, main peak A_2 with shoulder A_1) is known from the literature.[17,19] It is attributed to the sequential presence of amorphous solid water with a high desorption rate leading to peak A_1 and crystalline ice with a somewhat lower desorption rate leading to A_2. The standard interpretation for comparable experimental parameters is that amorphous solid water grows on top of the wetting layer and is then recrystallized during desorption to yield the crystalline ice peak. Thus, we conclude that in our desorption experiments on the flat (111) surface, the second water layer is amorphous and transforms into crystalline ice during heating.

Such a double-peak structure is not observed for the multilayer peak on the rippled surface. Instead, only the low-temperature shoulder, A_1, attributed to amorphous solid water is visible in the spectra (compare inset in Figure 3b). This is in accordance with the spectra in ref 21, although there, the absence of the shoulder was not interpreted as a step-related effect. The leading edge of this peak is virtually identical on the flat and rippled surfaces. We conclude that the molecules in this peak stem from almost identical environments on the surface; namely, amorphous solid water. The absence of a double peak structure on the rippled surface is good evidence that recrystallization is not possible on this highly stepped surface, as was assumed earlier.[44] This is understandable if one assumes that the critical nucleus for the formation of crystalline ice is larger than the terrace width, effectively preventing recrystallization. Furthermore, due to the small terrace size (and maybe a different structure of the film induced by the presence of steps), the first water layer cannot act as a template to facilitate crystallization. Bulk crystallization is not present here because the films are very thin.

5. Conclusions

In conclusion, our experiments on nanostructured Pt(111) have shown that steps have a 3-fold influence on the desorption of water form Pt(111): (i) Water is bound stronger to the steps than to the free terrace. This effect is most pronounced for (111) steps, where molecules are bound the strongest. (ii) On small terraces, desorption of the monolayer is of first order, which is in contrast to zero order, as observed on extended terraces. This finding can be rationalized by assuming that a condensed and a diluted phase coexist on wide terraces, whereas just a single phase is present on narrow ones. (iii) Multiple steps inhibit the crystallization of multilayer films, keeping all layers except the first one in an amorphous state until complete desorption. This can be due to the fact that the terraces are too small to house a nucleus for crystallization. Furthermore, the structure of the H_2O monolayer on the stepped surface may differ from the flat one, thereby not being able to act as a template for crystallization.

The results summarized above demonstrate that our approach to purposefully nanostructure the surface is an efficient method to probe the influence of well-defined step arrangements on molecular adsorption.

References and Notes

(1) Iwasita, T.; Nart, F. C. *Prog. Surf. Sci.* **1997**, *55*, 217.
(2) Marcus, P. *Electrochim. Acta* **1998**, *43*, 109.
(3) Lowe, D.; MacKenzie, A. R. *J. Atmos. Sol.-Terr. Phys.* **2008**, *70*, 13.
(4) Westley, M. S.; Baragiola, R. A.; Johnson, R. E.; Baratta, G. A. *Nature* **1995**, *373*, 405.
(5) Thiel, P. A.; Madey, T. E. *Surf. Sci. Rep.* **1987**, *7*, 211.
(6) Henderson, M. A. *Surf. Sci. Rep.* **2002**, *46*, 1.
(7) Morgenstern, M.; Pirug, G. In *Physics of Covered Solid Surfaces*; Bonzel, H. P., Ed.; Springer-Verlag: Berlin, 2006; *Vol. III-42-A5*, p 133.
(8) Glebov, A. L.; Graham, A. P.; Menzel, A. *Surf. Sci.* **1999**, *427-428*, 22.
(9) Glebov, A.; Graham, A. P.; Menzel, A.; Toennies, J. P. *J. Chem. Phys.* **1997**, *106*, 9382.
(10) Ogasawara, H.; Brena, B.; Nordlund, D.; Nyberg, M.; Pelmenschikov, A.; Pettersson, L. G. M.; Nilsson, A. *Phys. Rev. Lett.* **2002**, *89*, 276102.
(11) Haq, S.; Harnett, J.; Hodgson, A. *Surf. Sci.* **2002**, *505*, 121.
(12) Michealides, A.; Ranea, V. A.; de Andres, P. L.; King, D. A. *Phys. Rev. Lett.* **2003**, *90*, 216102.

(13) Daschbach, J. L.; Peden, B. M.; Smith, R. S.; Kay, B. D. *J. Chem. Phys.* **2004**, *120*, 1516.

(14) Kimmel, G. A.; Petrik, N. G.; Dohnálek, Z.; Kay, B. D. *Phys. Rev. Lett.* **2005**, *95*, 166102.

(15) Kimmel, G. A.; Petrik, N. G.; Dohnálek, Z.; Kay, B. D. *J. Chem. Phys.* **2007**, *126*, 114702.

(16) Morgenstern, M.; Müller, J.; Michely, T.; Comsa, G. *Z. Phys. Chem.* **1997**, *198*, 43.

(17) Dohnálek, Z.; Ciolli, R. L.; Kimmel, G. A.; Stevenson, K. P.; Smith, R. S.; Kay, B. D. *J. Chem. Phys.* **1999**, *110*, 5489.

(18) Zimbitas, G.; Haq, S.; Hodgson, A. *J. Chem. Phys.* **2005**, *123*, 174701.

(19) Kimmel, G. A.; Petrik, N. G.; Dohnálek, Z.; Kay, B. D. *J. Chem. Phys.* **2006**, *125*, 044713.

(20) Morgenstern, M.; Michely, T.; Comsa, G. *Phys. Rev. Lett.* **1996**, *77*, 703.

(21) Grecea, M. L.; Backus, E. H. G.; Riedmüller, B.; Eichler, A.; Kleyn, A. W.; Bonn, M. *J. Phys. Chem. B* **2004**, *108*, 12575.

(22) Meng, S.; Wang, E. G.; Gao, S. *Phys. Rev. B* **2004**, *69*, 195404.

(23) Jacobi, K.; Bedürftig, K.; Wang, Y.; Ertl, G. *Surf. Sci.* **2001**, *472*, 9.

(24) Jo, S. K.; Kiss, J.; Polanco, J. A.; White, J. M. *Surf. Sci.* **1991**, *253*, 233.

(25) Ogasawara, H.; Yoshinobu, J.; Kawai, M. *Chem. Phys. Lett.* **1994**, *231*, 188.

(26) Clay, C.; Haq, S.; Hodgson, A. *Phys. Rev. Lett.* **2004**, *92*, 046102.

(27) Bott, M.; Michely, T.; Comsa, G. *Rev. Sci. Instrum.* **1995**, *66* (8), 4135–4139.

(28) Hansen, H.; Redinger, A.; Messlinger, S.; Stoian, G.; Rosandi, Y.; Urbassek, H. M.; Linke, U.; Michely, T. *Phys. Rev. B* **2006**, *73*, 235414.

(29) Redinger, A.; Rosandi, Y.; Urbassek, H. M.; Michely, T. *Phys. Rev. B* **2008**, *77*, 195436.

(30) The adsorption rate in the center of the sample was determined by modeling the beam profile defined by the geometry of our dosing system as described in ref 38, where the relation of the total flux measured experimentally to the flux hitting the centre of the sample was derived. Furthermore, this analyis revealed that the flux at the edge of our 6-mm-wide sample is 30% of the one in the middle of the sample.

(31) Kalff, M.; Comsa, G.; Michely, T. *Phys. Rev. Lett.* **1998**, *81* (6), 1255–1258.

(32) Wagner, F. T.; Moylan, T. E.; Schmieg, S. J. *Surf. Sci.* **1988**, *195*, 403.

(33) Tränkenschuh, B.; Papp, C.; Fuhrmann, T.; Denecke, R.; Steinrück, H.-P. *Surf. Sci.* **2007**, *601*, 1108.

(34) Readhead, P. A. *Vacuum* **1962**, *12*, 203.

(35) Widdra, W.; Trischberger, P.; Frieβ, W.; Menzel, D.; Payne, S. H.; Kreuzer, H. J. *Phys. Rev. B* **1998**, *57*, 4111.

(36) Clay, C.; Haq, S.; Hodgson, A. *Chem. Phys. Lett.* **2004**, *388*, 89.

(37) Pérez-Maqueda, L. A.; Criadio, J. M. *J. Therm. Anal. Calorim.* **2000**, *60*, 909.

(38) Picolin, A. Wasser auf gestuften und ungestuften Platinflächen. M.S. Thesis, Universität zu Köln, Köln, Germany, 2008.

(39) Anderson, A. B. *Surf. Sci.* **1981**, *105*, 159.

(40) Meng, S.; Wang, E. G.; Gao, S. *Phys. Rev. B* **2004**, *69*, 195404.

(41) Siddiqui, H. R.; Guo, X.; Chorkendorff, I.; J, T.; Yates, J. *Surf. Sci.* **1987**, *191*, L813.

(42) Besocke, K.; Krahl-Urban, B.; Wagner, H. *Surf. Sci.* **1977**, *68*, 39.

(43) Eisenberg, D.; Kauzmann, W. *The Structure and Properties of Water*; Oxford University Press: New York, 1969.

(44) Backus, E. H. G.; Grecea, M. L.; Kleyn, A. W.; Bonn, M. *Phys. Rev. Lett.* **2004**, *92*, 236101.